Three-Dimensional Intravascular Ultrasound Assessment of Noninjured Edges of ß-Irradiated Coronary Segments

Ken Kozuma, Marco A. Costa, Manel Sabaté, I. Patrick Kay, Johannes P. A. Marijnissen, Veronique L. M. A. Coen, Pedro Serrano, Jurgen M. R. Ligthart, Peter C. Levendag and Patrick W. Serruys

Circulation 2000;102;1484-1489
Circulation is published by the American Heart Association. 7272 Greenville Avenue, Dallas, TX 72514
 Print ISSN: 0009-7322. Online ISSN: 1524-4539

Three-Dimensional Intravascular Ultrasound Assessment of Noninjured Edges of β-Irradiated Coronary Segments

Ken Kozuma, MD; Marco A. Costa, MD; Manel Sabaté, MD; I. Patrick Kay, MBChB; Johannes P.A. Marijnissen, PhD; Veronique L.M.A. Coen, MD; Pedro Serrano, MD; Jurgen M.R. Ligthart, BSc; Peter C. Levendag, MD, PhD; Patrick W. Serruys, MD, PhD, FACC

Background—The "edge effect," late lumen loss at the margins of the treated segment, has become an important issue in the field of coronary brachytherapy. The aim of the present study was to assess the edge effect in noninjured margins adjacent to the irradiated segments after catheter-based intracoronary β-irradiation.

Methods and Results—Fifty-three vessels were assessed by means of 3-dimensional intravascular ultrasound after the procedure and at 6- to 8-month follow-up. Fourteen vessels (placebo group) did not receive radiation (sham source), whereas 39 vessels were irradiated. In the irradiated group, 48 edges (5 mm in length) were identified as noninjured, whereas 18 noninjured edges were selected in the placebo group. We compared the volumetric intravascular ultrasound measurements of the noninjured edges of the irradiated vessels with the fully irradiated nonstented segments (IRS, n=27) (26-mm segments received the prescribed 100% isodose) and the noninjured edges of the vessels of the placebo patients. The lumen decreased (6 mm^3) in the noninjured edges of the irradiated vessels at follow-up ($P=0.001$). We observed a similar increase in plaque volume in all segments: noninjured edges of the irradiated group (19.6%), noninjured edges of the placebo group (21.5%), and IRS (21.0%). The total vessel volume increased in the IRS in the 3 groups. No edge segment was subject to repeat revascularization.

Conclusions—The edge effect occurs in the noninjured margins of radiation source train in both irradiated and placebo patients. Thus, low-dose radiation may not play an important role in this phenomenon, whereas nonmeasurable device injury may be considered a plausible alternative explanation. **(*Circulation*. 2000;102:1484-1489.)**

Key Words: brachytherapy ■ angioplasty ■ ultrasonics

The "edge effect," a lumen loss at the segments adjacent to the treated site, is a new phenomenon in the field of interventional cardiology. Although it may also occur after conventional treatment (ie, stent implantation),[1,2] it has become an important issue after the introduction of intracoronary brachytherapy in clinical practice.

Recently, the edge effect was reported in patients who received radioactive stents with intermediate activity (3 to 12 μCi). Neointimal formation was inhibited in a dose-dependent manner within the stented area, but proliferation and unfavorable remodeling were demonstrated at the stent margins .[3] The authors dubbed this angiographic finding as the "candy-wrapper" effect. Further, the edge effect has been observed in patients treated by means of catheter-based β-radiation.[4,5] In a 3-dimensional (3-D) volumetric intravascular ultrasound (IVUS) investigation, our group observed a decrease in lumen volume at the edges of the irradiated segment due to an increase in plaque volume not accommodated by vessel enlargement.[5] In all 3 reports, the authors hypothesized that the edge effect was due to the combination of low-dose radiation and balloon-induced injury in the segments adjacent to the irradiated site. Indeed, the potential stimulatory effect of low-dose radiation after injury has been demonstrated in animal studies.[6,7]

In consideration that the coronary segments adjacent to the irradiated site will invariably receive a lower dose of radiation to some extent, an important issue remains to be clarified: Does the edge effect also occur in noninjured segments? To address this issue, we (1) assessed the midterm (6 to 8 months) geometrical change of the noninjured edge segments in the irradiated coronary vessels and (2) compared these edge segments with both irradiated segments (IRS) and nonirradiated (sham source), noninjured coronary segments by means of a volumetric 3-D IVUS assessment.

Methods

Study Population

From April 1997 to March 1999, 56 de novo lesions of 50 patients were treated with catheter-based intracoronary β-radiation with the Beta-Cath System (Novoste Corp). IVUS analyses of 10 vessels (7

Received February 7, 2000; revision received April 20, 2000; accepted May 8, 2000.

From the Thoraxcenter (K.K., M.A.C., M.S., I.K., P.S., J.M.R.L., P.W.S.), University Hospital Rotterdam Dijkzigt, the Netherlands; and Daniel den Hoed Cancer Center (J.P.A.M., V.L.M.A.C., P.C.L.), Rotterdam, the Netherlands.

Correspondence to P.W. Serruys, MD, PhD, FACC, Department of Interventional Cardiology, University Hospital Rotterdam Dijkzigt, Thoraxcenter Bd408, Dr Molewaterplein 40, 3015 GD Rotterdam, the Netherlands. E-mail serruys@card.azr.nl

***Circulation* is available at http://www.circulationaha.org**

patients) were not included in this study due to the implantation of multiple stents overlapping outside the irradiated area. In addition, 3-D IVUS analysis was not carried out either after the procedure or at follow-up in 7 vessels (7 patients): 2 had severe restenosis (1 diffuse restenosis, 1 in-stent restenosis, not related to their edges), 3 presented with thrombotic occlusion, and 2 other patients without recurrent angina refused follow-up angiography. The placebo group consists of 14 patients who were successfully treated with conventional balloon angioplasty or single-stent implantation during the same period. In these patients, the radiation delivery catheter was also introduced into the target coronary arteries, but a dummy source train was used instead of radioactive source according to randomization.

Thus, the study population consists of 36 irradiated patients (39 vessels) and 14 nonirradiated placebo patients (14 vessels) who underwent successful 3-D ECG-gated IVUS analysis immediately after the procedure and at follow-up. Patients were treated due to ischemia-related symptoms or positive stress testing. Those with myocardial infarction within 72 hours before the treatment or a left ventricular ejection fraction of <0.30 were not included in the study. Angiographic inclusion criteria consist of a reference vessel diameter of >2.5 mm and <4.0 mm and a lesion length of <20 mm.

The Medical Ethics Committee of the University Hospital Dijkzigt approved the use of intracoronary radiation. All patients gave written informed consent.

Radiotherapy System

The source train of the Beta-Cath System consists of a series of 12 independent cylindrical seeds that contain pure β-emitting $^{90}Sr/^{90}Y$ and is bordered by 2 gold markers (30 mm in length). The longitudinal distance of the "full" prescribed dose (100% isodose) coverage measured with radiochromic films is ≈26 mm (Novoste Corp, data on file, personal communication). The profile of the catheter is 5F, and the source train is not centered.

Procedure

All patients received aspirin (250 mg/d) and heparin IV (10 000 IU) before the procedure, whereas stented patients also received ticlopidine (250 mg/d) for 30 days. Heparin was administered to maintain the activated clotting time at >300 seconds. Balloon angioplasty (BA) was performed according to standard clinical practice. After successful angioplasty, intracoronary β-irradiation was performed as previously described,[8] and repeat angiography and IVUS motorized pullback were carried out. If stenting was indicated due to a residual stenosis of >30% diameter stenosis or dissection, a stent was implanted with high-pressure postdilatation and IVUS guidance. Finally, repeat angiography and IVUS were carried out. Intracoronary nitrates were administered immediately before each of the IVUS pullbacks. At follow-up (6 to 8 months), further IVUS analysis of the treated vessel was performed. The prescribed doses were 0 Gy (14 vessels), 12 Gy (8 vessels), 14 Gy (9 vessels), 16 Gy (9 vessels), and 18 Gy (13 vessels).

IVUS Image Acquisition Analysis System

The methodology of 3-D IVUS image acquisition and quantitative analysis has been described previously.[5,9] In brief, the segment subject to 3-D reconstruction was examined with a 30-MHz single-element mechanical transducer IVUS system (ClearView, CVIS; Boston Scientific Corp). ECG-gated 3-D IVUS image acquisition and digitization were performed with a computerized workstation (EchoScan; TomTec).[10] IVUS images were acquired that coincided with the peak of the R wave, which eliminates the artifacts caused by the movement of the heart during the cardiac cycle. The IVUS transducer was withdrawn in 0.2-mm steps with an ECG-triggered pullback device.

A Microsoft Windows–based contour detection system, developed at the Thoraxcenter, was used for 3-D volumetric quantification.[11] This program constructed 2 longitudinal sections from the data set and identified the contours that correspond to the lumen, media, or stent boundaries. Volumetric data were automatically

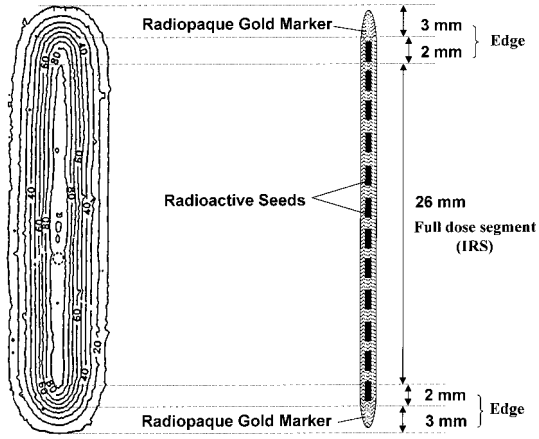

Figure 1. Isodose rate contour map and radiation source train. Left, Isodose rate contour map at a depth of 1.89 mm (10 mGy/s contour intervals) as described by The National Institute of Standards and Technology. This depth (1.89 mm) illustrates an isodose model to resemble radius of coronary artery wall. Longitudinal dose fall-off may be extrapolated from this graphic. Right, Radiation source train. Central part of source train (26 mm) receives approximately full dose.

calculated with the following formula: $V=\Sigma_{i=1}^{n} A_i \times H$, where V is volume; A is the area of external elastic membrane, lumen, or plaque in a given cross-sectional ultrasound image; H is slice thickness of the cross section (0.2 mm); and n is the number of digitized cross-sectional images that encompass the volume to be measured.[11] Offline analyses were performed by 3 independent experienced analysts (K.K., M.C., M.S.) who checked and edited all of the contours of the planar images. The accuracy of this method has been validated in vitro (phantom) and in vivo.[12] Intraobserver and interobserver variabilities of this system have also been determined in clinical protocols.[9] Intraobserver variability assessed with analysis of the IVUS volumetric studies at intervals of ≥3 months has been reported: −0.4±1.1% in lumen volume, −0.4±0.6% in total vessel volume, and −0.3±1.0% in plaque volume with ECG-gated motorized pullback.

The methodology to define the treated segment in the irradiated patients has been previously described.[5] An angiogram was performed during contrast injection after positioning of the delivery catheter, and the relation between anatomic landmarks and the 2 radiopaque markers of the radiation source was noted. Typically, the aorto-ostial junction, side branches, stent, or a combination were used as landmarks. During the subsequent IVUS imaging pullback, this reference point was recognized and used for selection of the 30-mm-long segment where the radiation source train was placed and both 3-mm distal and proximal edges (36-mm-long segment in total). At follow-up, correct matching of the region of interest was performed by comparing the longitudinal reconstruction with that after the procedure. The longitudinal distance of the 100% isodose is ≈26 mm, as illustrated in Figure 1. Thus, we defined the target irradiated segments (IRS) as the segments covered by the 26-mm full-activity central portion of the radiation source train and the edges of the IRS as the adjacent (distal and proximal) 5-mm coronary segments, which consisted of 2 mm inside the gold markers and 3 mm proximal or distal including the gold markers (Figure 1). IRS-containing stents (n=12) were excluded from the analysis.

The 5-mm edge segments selected in our study received low-dose radiation because β-emitting $^{90}Sr/^{90}Y$ source has an acute fall-off of delivery dose related to the distance.[13,14] For instance, the highest prescribed dose in our study was 18 Gy, and the calculated longitudinal dose per millimeter from the 100% isodose boundary is expected to be 15.5±1.0 Gy at 1 mm, 11.0±1.0 Gy at 2 mm, 5.5±0.5 Gy at 3 mm, 2.4±1.0 Gy at 4 mm, and <1 Gy at 5 mm.

To select the noninjured segments, all locations of deflated balloons, stent delivery system, inflated balloons, and radiation

source train were recorded in the angiogram. The deflated balloon, stent delivery system, and delivery radiation catheter were also filmed during contrast injection. All angioplasty balloons used in this study had 2 radiopaque markers in both extremities. Each cine frame of angiograms that show the position of inflated balloon, deflated balloon markers, stent delivery system, and the radiation source train can be displayed simultaneously on the separated screen during offline analysis with the Rubo DICOM Viewer (Rubo Medical Imaging). A continuous ECG recording was also displayed, which permitted the selection of images in the same moment of the cardiac cycle. By identifying the relationship between landmarks and device radiopaque markers, we were able to select only the balloon- or stent-injured fully irradiated coronary segment (covered by the 26-mm central portion of the radioactive source train). Therefore, all of the injured edge segments were excluded. At follow-up, it was also possible to determine the noninjured edge segments according to the same method, because all of the follow-up cine films were taken in the same views as before and after the procedure. This angiographic analysis was performed independently by 2 cardiologists (K.K., M.C.). Only the edges, which both investigators regarded as noninjured segments, were finally considered to be noninjured edges. There was only 10% disagreement in the definition of injured irradiated edge segment with this methodology. The 3-mm stent edges were also considered to be injured segments, because the balloon of the stent delivery system may protrude ≈2 to 3 mm outside the stent.

Quantitative 3-D IVUS Analysis

Total vessel volume (TVV) determined with external elastic membrane boundaries and lumen volume (LV) were measured. Plaque volume (PV) was automatically calculated by subtracting LV from TVV. To assess the volumetric changes of the vessel structures after 6 to 8 months, the Δ value for each measurement was calculated (Δ=follow-up−postprocedure). To eliminate the influence of the vessel size and the length of the analyzed segment, which affects volume calculations, percent Δ change (Δ volume/postprocedure volume) was also calculated.

"Remodeling" was defined as a continuous process that involved any positive or negative changes in TVV.[15] In the present study, remodeling of the vessel wall was considered when TVV increased or decreased compared with postprocedure measurements by ≥2 SDs (±1.3%) of the intraobserver variability. By using this technique, the potential intrinsic error of the method may be avoided.[16,17]

Statistical Analysis

Quantitative data are presented as mean±SD. Comparisons between postprocedure and follow-up IVUS parameters were compared by paired Student's *t* test. Comparisons of the IVUS data among the 3 groups (noninjured edge of the irradiated vessels, IRS, and noninjured edge of the placebo group) were performed by 1-way ANOVA. Bonferroni's test was applied for comparison between groups. The difference between proximal and distal edges was compared by 2-tailed Student's *t* test. The correlation between percent change in plaque volume and prescribed dose, corrected by the mean total vessel area at the edges based on 3-D IVUS measurement, were tested by Pearson's correlation. A value of $P<0.05$ was considered statistically significant.

Results

Baseline clinical, demographic, and angiographic characteristics were similar between irradiated and placebo patients (Table 1). No myocardial infarction or death was observed in this population during the 6- to 8-month follow-up. Target lesion revascularization was performed after follow-up angiography in 6 vessels in the irradiated group (16%) and 2 vessels in placebo group (14%). The noninjured edges were not involved in any of the restenotic lesions that required further intervention in both groups.

TABLE 1. Clinical and Lesion Characteristics

	Irradiated Group (n=36)	Placebo Group (n=14)	*P*
Clinical			
Age, y	57±9	57±9	NS
Male, n (%)	27 (75)	13 (93)	NS
Coronary risk, n (%)			
Smoking history	26 (72)	11 (79)	NS
Dyslipidemia	21 (58)	7 (50)	NS
Diabetes mellitus	4 (11)	2 (14)	NS
Hypertension	14 (39)	2 (14)	NS
Family history	17 (47)	7 (50)	NS
Unstabele angina, n (%)	13 (36)	5 (36)	NS
Multivessel disease, n (%)	12 (33)	1 (7)	NS
Lesions			
Treated lesions, n	39	14	
Vessel location, n (%)			
LAD	15 (38)	6 (43)	
LCx	10 (26)	3 (21)	NS
RCA	14 (36)	5 (36)	
Stent implantation	12 (31)	7 (39)	NS
Maximum balloon size, mm	3.63±0.6	3.63±0.5	NS

LAD indicates left anterior descending coronary artery; LCx, left circumflex coronary artery; and RCA, right coronary artery.

Forty-eight edge segments (20 distal and 28 proximal edges) and 27 irradiated segments without stents were analyzed with 3-D volumetric IVUS in the irradiated population. Thirty edges were excluded from this analysis. The reasons for exclusion were ostial location of the proximal end of the source (n=11), overlapping of 1 of the edges with large side branches (>2.0-mm diameter) (n=5) or stent (n=6), injury of 1 of the edges by angioplasty balloon (n=4), and lack of follow-up IVUS analysis with the ECG-gated motorized pullback (n=4).

In the placebo group, 18 edges (11 distal and 7 proximal edges) were examined with 3-D volumetric IVUS. Ten edges were excluded because of ostial location of the proximal end of the dummy source (n=6), overlapping of 1 of the edges with large side branches (n=1), and injury of 1 of the edges (n=3).

All 3-D IVUS volumetric measurements of PV, TVV, and LV are listed in Table 2. Some degree of atherosclerosis (≥15% plaque burden) was observed in most of the noninjured edges in the postprocedure IVUS analysis, but no edge (radiation or placebo group) had >50% plaque burden. Compared with the postprocedure measurement, there was a significant increase in PV in the noninjured edges of the irradiated vessels ($\Delta PV=4$ mm^3) at follow-up. Because TVV on average decreased by -2 mm^3 (P=NS), LV decreased at follow-up in the noninjured edge of the irradiated vessels ($\Delta LV=-6$ mm^3). In the placebo group, there also was a tendency of plaque increase at follow-up ($\Delta PV=4$ mm^3) in the noninjured edge of the placebo group ($P=0.06$).

TABLE 2. Volumetric Measurement of 3-D IVUS

	IRS (n=27)		Noninjured Edge Irradiated Vessel (n=48)		Noninjured Edge Placebo (n=18)	
	Post	Follow-Up	Post	Follow-Up	Post	Follow-Up
PV, mm^3	196±56	234±69*	32±15	36±16*	27±14	31±15†
TVV, mm^3	441±136	480±159‡	81±32	79±31	65±21	67±24
LV, mm^3	245±101	247±114	48±22	42±21§	38±15	37±16

*$P<0.001$, †$P=0.06$, ‡$P=0.004$, §$P=0.001$.
Post indicates post procedure.

Comparisons among the geometric changes of the 3 groups (IRS, noninjured edges of the irradiated vessels, and noninjured edges of the placebo group) are demonstrated in Figure 2. The percent increase in PV was similar among IRS, noninjured edges of the irradiated vessels, and those of placebo group (+21.0% versus +19.6% versus +21.5%, respectively). TVV increased in IRS significantly among the 3 groups (+9.4% at IRS; −1.0% at noninjured edges of the irradiated vessels; +3.8% at noninjured edge of the placebo, $P=0.021$). The difference was observed only between IRS and noninjured edges of the irradiated vessels by post hoc test ($P=0.017$). Percent changes in LV were different (+1.7% versus −10.0% versus −2.5%, respectively, $P=0.049$) among the 3 groups. LV tended to decrease in the noninjured edges of irradiated patients compared with IRS ($P=0.053$).

Comparisons between the geometric changes of the proximal and distal noninjured edges are shown in Figure 3. Although there was no statistical difference in geometric change between distal and proximal edges, the percent increase in PV tended to be greater in the proximal edges than in the distal edges (+27.0% versus +9.2%).

Finally, there was no correlation between the percent increase in PV and prescribed dose corrected by mean vessel area at the edges ($P=0.76$, $r=-0.046$).

Discussion

This is the first study to investigate the geometric changes of noninjured margins of endovascular catheter–based radiation therapy. The edge effect, a decrease in lumen volume at follow-up, was observed in the noninjured edges of the irradiated vessels (Table 2). However, plaque proliferation induced by low-dose radiation may not fully account for the occurrence of this phenomenon, because plaque volume increased similarly in the noninjured edges of placebo group (Figure 2).

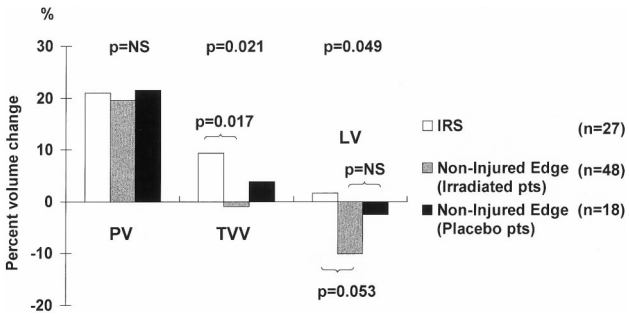

Figure 2. Comparisons of percent volume changes among IRS and noninjured edges of both irradiated and placebo patients.

Lumen loss was observed in the noninjured edges of the irradiated group. The decrease in LV observed in these edges was mainly due to the lack of positive vessel remodeling (ie, no remodeling)[15] to accommodate the plaque increase, which occurred similarly in all analyzed segments. Likewise, the lumen also decreased (2.5%) in the noninjured edges of the control group, but in this case we observed some degree of vessel enlargement (3.8% increase in TVV). The facilitation of favorable positive remodeling[15] promoted by radiation may explain the preservation of lumen dimension (1.7% increase in LV) observed only in the IRS. Both phenomena, positive remodeling stimulated by intravascular radiation after balloon angioplasty and different patterns of vascular remodeling (positive, negative, or no remodeling) in nonirradiated coronary segments, have been reported previously.[5,18–20]

Although the stimulatory effect of low-dose radiation on plaque proliferation has been demonstrated in injured animal arteries,[6,7] no enhanced plaque growth was observed in the noninjured edges compared with placebo. Plausible explanations for the PV increase in the noninjured edges of both irradiated and placebo groups would be the nonmeasurable vessel injuries caused by the guiding catheter (ie, deep engagement) during the procedure or the devices that cross coronary segments (guidewires, stents, balloons, IVUS catheter, and the 5F radiation delivery catheter). Indeed, a tendency of greater plaque increase was observed in the proximal edges, where these types of injury may occur more frequently, although it might have been hypothesized that the 5F radiation delivery catheter could induce higher injury to the distal part due to the tapering of the vessel.

It is nevertheless important to emphasize that this phenomenon occurred in segments not injured by balloon inflation, which may highlight the importance of the use of a less aggressive approach: the avoidance of deep catheter engagement, guidewire entrapment, or rough device introduction against resistance, especially in tortuous vessels. To avoid device-induced injury, low-profile and more flexible radiation delivery catheters will be a worthy development for catheter-based brachytherapy.

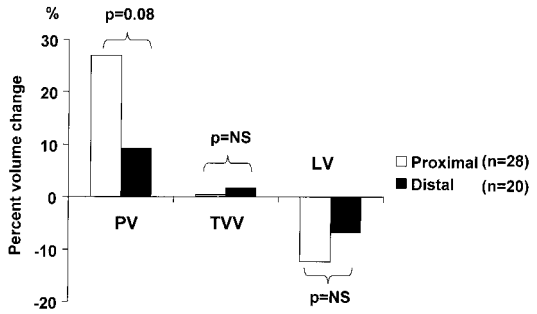

Figure 3. Comparisons of percent volume changes between proximal and distal edges in irradiated vessels.

The 10% lumen loss observed in the edges of the irradiated vessels had no clinical impact, because no repeat revascularization was performed due to noninjured edge stenosis. However, this finding may have important implications if plaque grows locally (ie, 1- or 2-mm short segment) or lumen reduction occurs in small or diffuse diseased vessels in the general treated population.

In conclusion, the edge effect occurs after catheter-based β-irradiation in the margins that were not injured by balloon inflation. This phenomenon was basically due to plaque growth without vessel remodeling. Our findings suggest that low-dose radiation may not be implicated as the cause of the edge effect and that clinically nonassessable device injury would be considered as a plausible explanation for this phenomenon. Clinically, the edge effect observed in our midterm follow-up IVUS study did not represent a drawback of the catheter-based intracoronary β-radiation.

Study Limitations

The number of the placebo patients was relatively small. However, the use of the "state-of-the art" 3-D IVUS technology in our study may overcome this limitation, because a smaller number of patients are necessary to demonstrate statistical differences in studies with volumetric IVUS parameters.[21]

Minor inaccuracy in the selection of the segments of interest cannot be completely ruled out, although the methodology applied in the present study was the most appropriate at this time. Ideally, intervention devices that incorporate IVUS imaging elements would be the solution for this drawback.

In a human clinical study, it is not possible to quantify the degree of vessel injury (ie, injury score),[22] which would provide further insight about this issue.

The actual dose received at irradiated and edge segments may have some implications in the geometric changes of the edges and would be interpreted as a limitation of our investigation. However, the study was not aimed at establishing a threshold of dose to be delivered to the irradiated target site, because an adjacent coronary segment will invariably receive low dose of radiation.

The 6- to 8-month follow-up period of this study may be too short to demonstrate the long-term arterial response to the radiation treatment. Increased risk of accelerated atherosclerosis progression after radiation therapy for malignancy has been reported.[23–27] Further, a recent report has shown that continuous low-dose rate irradiation delivered by radioactive stent promotes "atheromatous" neointimal formation.[28] Therefore, a question still remains to be elucidated: Does endovascular radiation have any influence on the progression of atherosclerosis, especially in the adjacent nontarget irradiated segments?

Acknowledgments

The Wenckebach Prize was awarded to Dr Serruys by the Dutch Heart Foundation for brachytherapy research. Dr Kay is supported by The National Heart Foundation of New Zealand. The authors are indebted to Eric Boersma, PhD, for assistance in statistics.

References

1. Hoffmann R, Mintz GS, Dussaillant GR, et al. Patterns and mechanisms of in-stent restenosis: a serial intravascular ultrasound study. *Circulation*. 1996;94:1247–1254.
2. Ikari Y, Hara K, Tamura T, et al. Luminal loss and site of restenosis after Palmaz-Schatz coronary stent implantation. *Am J Cardiol*. 1995;76:117–120.
3. Albiero R, Adamian M, Kobayashi N, et al. Short- and intermediate-term results of ^{32}P radioactive β-emitting stent implantation in patients with coronary artery disease: the Milan Dose-Response Study. *Circulation*. 2000;101:18–26.
4. Sabate M, Kay IP, Gijzel AL, et al. Compassionate use of intracoronary beta-irradiation for treatment of recurrent in-stent restenosis. *J Invas Cardiol*. 1999;11:582–588.
5. Sabate M, Serruys PW, van der Giessen WJ, et al. Geometric vascular remodeling after balloon angioplasty and beta- radiation therapy: a three-dimensional intravascular ultrasound study. *Circulation*. 1999;100:1182–1188.
6. Schwartz RS, Koval TM, Edwards WD, et al. Effect of external beam irradiation on neointimal hyperplasia after experimental coronary artery injury. *J Am Coll Cardiol*. 1992;19:1106–1113.
7. Weinberger J, Amols H, Ennis RD, et al. Intracoronary irradiation: dose response for the prevention of restenosis in swine. *Int J Radiat Oncol Biol Phys*. 1996;36:767–775.
8. King SB 3rd, Williams DO, Chougule P, et al. Endovascular beta-radiation to reduce restenosis after coronary balloon angioplasty: results of the Beta Energy Restenosis Trial (BERT). *Circulation*. 1998;97:2025–2030.
9. von Birgelen C, de Vrey EA, Mintz GS, et al. ECG-gated three-dimensional intravascular ultrasound: feasibility and reproducibility of the automated analysis of coronary lumen and atherosclerotic plaque dimensions in humans. *Circulation*. 1997;96:2944–2952.
10. Bruining N, von Birgelen C, de Feyter PJ, et al. ECG-gated versus nongated three-dimensional intracoronary ultrasound analysis: implications for volumetric measurements. *Cathet Cardiovasc Diagn*. 1998;43:254–260.
11. Li W, von Birgelen C, Di Mario C, et al. Semi-automated contour detection for volumetric quantification of intracoronary ultrasound. *Comput Cardiol*. 1994;277–280.
12. von Birgelen C, Di Mario C, Li W, et al. Morphometric analysis in three-dimensional intracoronary ultrasound: an in vitro and in vivo study performed with a novel system for the contour detection of lumen and plaque. *Am Heart J*. 1996;132:516–527.
13. Soares CG, Halpern DG, Wang CK. Calibration and characterization of beta-particle sources for intravascular brachytherapy. *Med Phys*. 1998;25:339–346.
14. Amols HI, Zaider M, Weinberger J, et al. Dosimetric considerations for catheter-based beta and gamma emitters in the therapy of neointimal hyperplasia in human coronary arteries. *Int J Radiat Oncol Biol Phys*. 1996;36:913–921.
15. Schwartz RS, Topol EJ, Serruys PW, et al. Artery size, neointima, and remodeling: time for some standards. *J Am Coll Cardiol*. 1998;32:2087–2094.
16. Kearney PP, Ramo MP, Shaw TR, et al. Analysis of reproducibility of reference lumen quantitation with intravascular ultrasound in stented coronary arteries. *Cathet Cardiovasc Diagn*. 1997;40:1–7.
17. Sabate M, Kay IP, de Feyter PJ, et al. Remodeling of atherosclerotic coronary arteries varies in relation to location and composition of plaque. *Am J Cardiol*. 1999;84:135–140.

18. Costa MA, Sabate M, Serrano P, et al. The effect of 32P beta-radiotherapy on both vessel remodeling and neointimal hyperplasia after coronary balloon angioplasty and stenting: a three-dimensional intravascular ultrasound investigation. *J Invas Cardiol*. 2000;12: 113–120.
19. Kakuta T, Currier JW, Haudenschild CC, et al. Differences in compensatory vessel enlargement, not intimal formation, account for restenosis after angioplasty in the hypercholesterolemic rabbit model. *Circulation*. 1994;89:2809–2815.
20. Mintz GS, Popma JJ, Pichard AD, et al. Arterial remodeling after coronary angioplasty: a serial intravascular ultrasound study. *Circulation*. 1996;94:35–43.
21. Mehran R, Mintz GS, Hong MK, et al. Validation of the in vivo intravascular ultrasound measurement of in-stent neointimal hyperplasia volumes. *J Am Coll Cardiol*. 1998;32:794–799.
22. Schwartz RS, Huber KC, Murphy JG, et al. Restenosis and the proportional neointimal response to coronary artery injury: results in a porcine model. *J Am Coll Cardiol*. 1992;19:267–274.
23. Moritz MW, Higgins RF, Jacobs JR. Duplex imaging and incidence of carotid radiation injury after high-dose radiotherapy for tumors of the head and neck. *Arch Surg*. 1990;125:1181–1183.
24. Reinders JG, Heijmen BJ, Olofsen-van Acht MJ, et al. Ischemic heart disease after mantlefield irradiation for Hodgkin's disease in long-term follow-up. *Radiother Oncol*. 1999;51:35–42.
25. Hancock SL, Tucker MA, Hoppe RT. Factors affecting late mortality from heart disease after treatment of Hodgkin's disease. *JAMA*. 1993; 270:1949–1955.
26. Stewart JR, Fajardo LF, Gillette SM, et al. Radiation injury to the heart. *Int J Radiat Oncol Biol Phys*. 1995;31:1205–1211.
27. Friedlander AH, Eichstaedt RM, Friedlander IK, et al. Detection of radiation-induced, accelerated atherosclerosis in patients with osteoradionecrosis by panoramic radiography. *J Oral Maxillofac Surg*. 1998;56: 455–459.
28. Carter AJ, Scott D, Bailey L, et al. Dose-response effects of ^{32}P radioactive stents in an atherosclerotic porcine coronary model. *Circulation*. 1999;100:1548–1554.